SUPPORTING INFORMATION

Theoretical Screening of P-block Single Atoms Anchored on g-C_3N_4 for NO Reduction to NH_3

Qingchao Fang[a,b], Yun Han[c], Xuxin Kang[d], Md Tarikal Nasir[a], Dimuthu Wijethunge[e], Cheng Yan[f], Anthony P. O' Mullane[f], Hanqing Yin[a,g*], Aijun Du[a,g]

[a] School of Chemistry and Physics, Queensland University of Technology (QUT), Gardens Point Campus, Brisbane, 4001, Australia

[b] School of Petroleum and Chemical Engineering, Dongying Vocational College, Dongying, P.R. China

[c] School of Engineering and Built Environment, Queensland Micro- and Nanotechnology Centre, Griffith University, Nathan Campus, Nathan, Queensland 4111, Australia

[d] School of Physical Science and Technology, Ningbo University, Ningbo, P.R. China

[e] School of Engineering, University of Southern Queensland, 37 Sinnathamby Blvd, Springfield Central QLD 4300, Australia

[f] School of Mechanical, Medical and Process Engineering, Queensland University of Technology (QUT), Brisbane, QLD 4001, Australia

[g] QUT Centre for Materials Science, Queensland University of Technology, Gardens Point Campus, Brisbane, 4001, Australia

*Corresponding author.

E-mail: hanqing.yin@connect.qut.edu.au (H.Yin)

Computation details

The Gibbs free energy change (ΔG) for the neighbouring elemental step of NORR and HER is based on the following[1]:

$$\Delta G = \Delta E + \Delta E_{ZPE} - T\Delta S \quad \text{(S1)}$$

Where ΔE is the energy difference between the energies of neighbouring optimized intermediates obtained from DFT calculations at 0K, ΔE_{ZPE} is the zero-point energy. T equals 298.15 K and ΔS is the change of entropy. The zero-point energy and entropies of the intermediates were computed from vibrational frequencies and post-processed by the VASPKIT package.[2] As for the gases such as NO, H_2, NH_3 and H_2O, the corresponding enthalpies and entropies were post-processed by VASPKIT as well. The chemical potential of ($H^+ + e^-$) at standard conditions equals as (1/2* G_{H_2} – neU), where n is the number of electrons involved in the reaction and U is the electrode potential relative to the RHE, and the standard conditions mean pH=0 and T=298.15 K.

The stable anchoring of SAC onto the g-C_3N_4 is a prerequisite for the NO reduction reaction process, which is validated by the formation energy as below,

$$E_f = E_{*SAC} - E_* - E_{SAC\text{-}bulk}/n \quad \text{(S2)}$$

Where E_{*SAC}, E_*, and $E_{SAC\text{-}bulk}$ represent the total energies of SAC/g-C_3N_4, g-C_3N_4 and SAC in the bulk phase, respectively, n is the number of bulk atoms per unit cell.

For the assessment of electrochemical stability, the dissolution energy of p-atom-doped C_3N_4 layer was evaluated based on the formation energy E_f and dissolution potential U_{diss} as shown below,

$$U_{diss} = U^o_{diss}(metal,bulk) - E_f/ne \quad \text{(S3)}$$

where $E_{SAC}/_{C_3N_4}$, E_{SAC} and $E_{C_3N_4}$ represents the p-block-doped g-C_3N_4 monolayer, the energies of the metal atom in the most stable structure and g-C_3N_4 monolayer, respectively. $U^o_{diss}(metal,bulk)$ stands for the standard dissolution potential of the p-block bulk and n means the number of the electrons involved.

As shown in **Fig S1**, the NO adsorption may not be adsorbed onto the SAC site. Since the study focuses on the SAC reactive site, thus the Si-based and In-based SAC are excluded for further consideration.

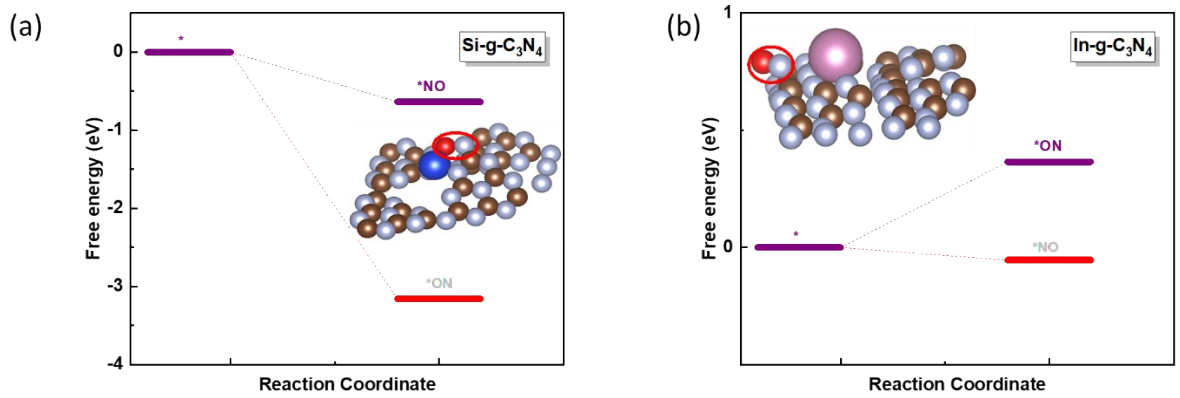

Fig S1. The NO adsorption free energy of NORR on Si@g-C_3N_4 and In@g-C_3N_4 are displayed, where these two thermodynamically favourable configurations are excluded due to no reactive site on SAC.

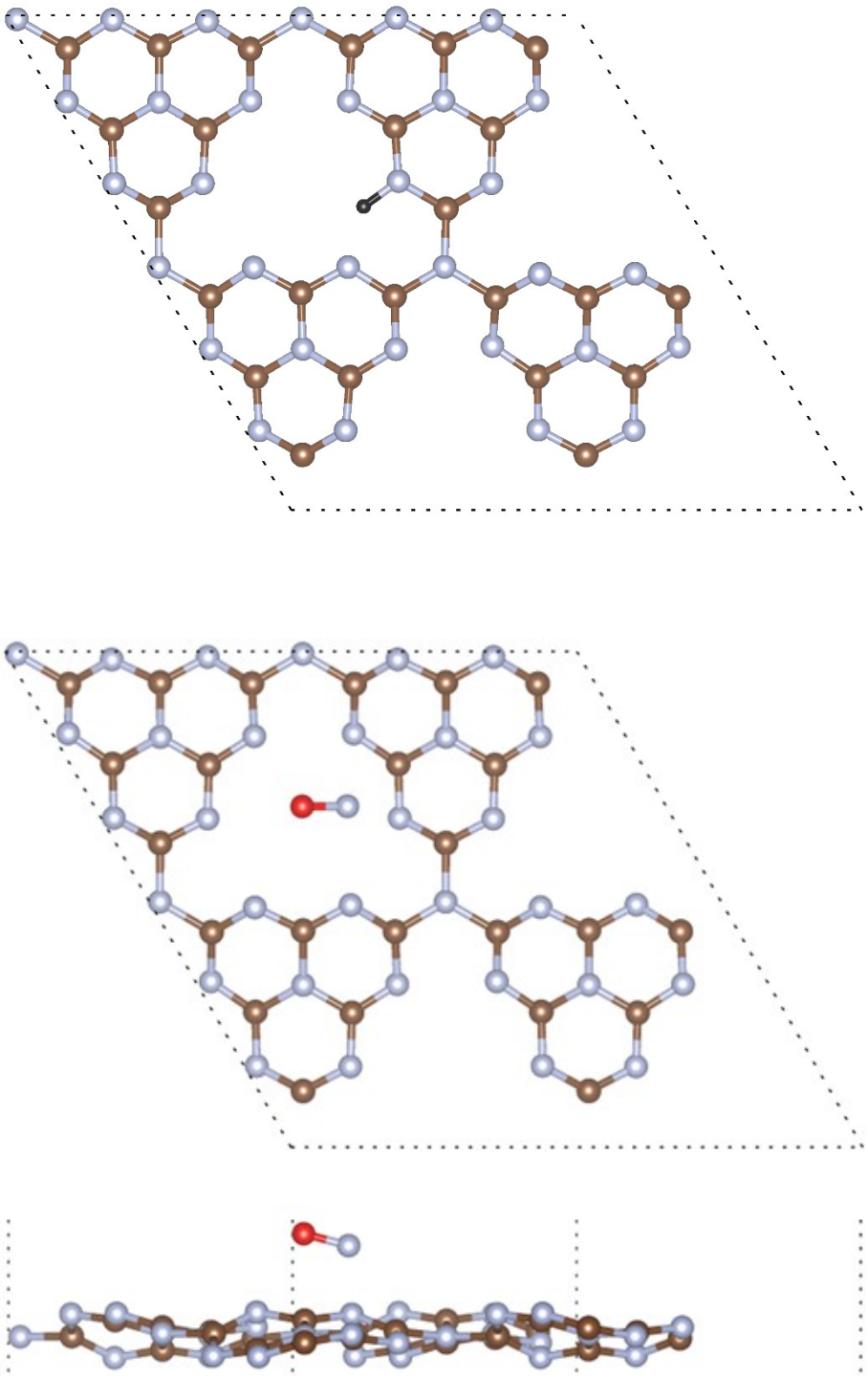

Fig S2. top: optimized adsorption configuration of proton on pure g-C_3N_4;

bottom: optimized adsorption configuration of NO on pure g-C_3N_4.

Colour map: silver—N; brown—C; red—O.

The Gibbs free energy profile of SACs on g-C_3N_4 was shown in **Fig S3**, where the grey intermediates mean the desorption from the SAC reactive site.

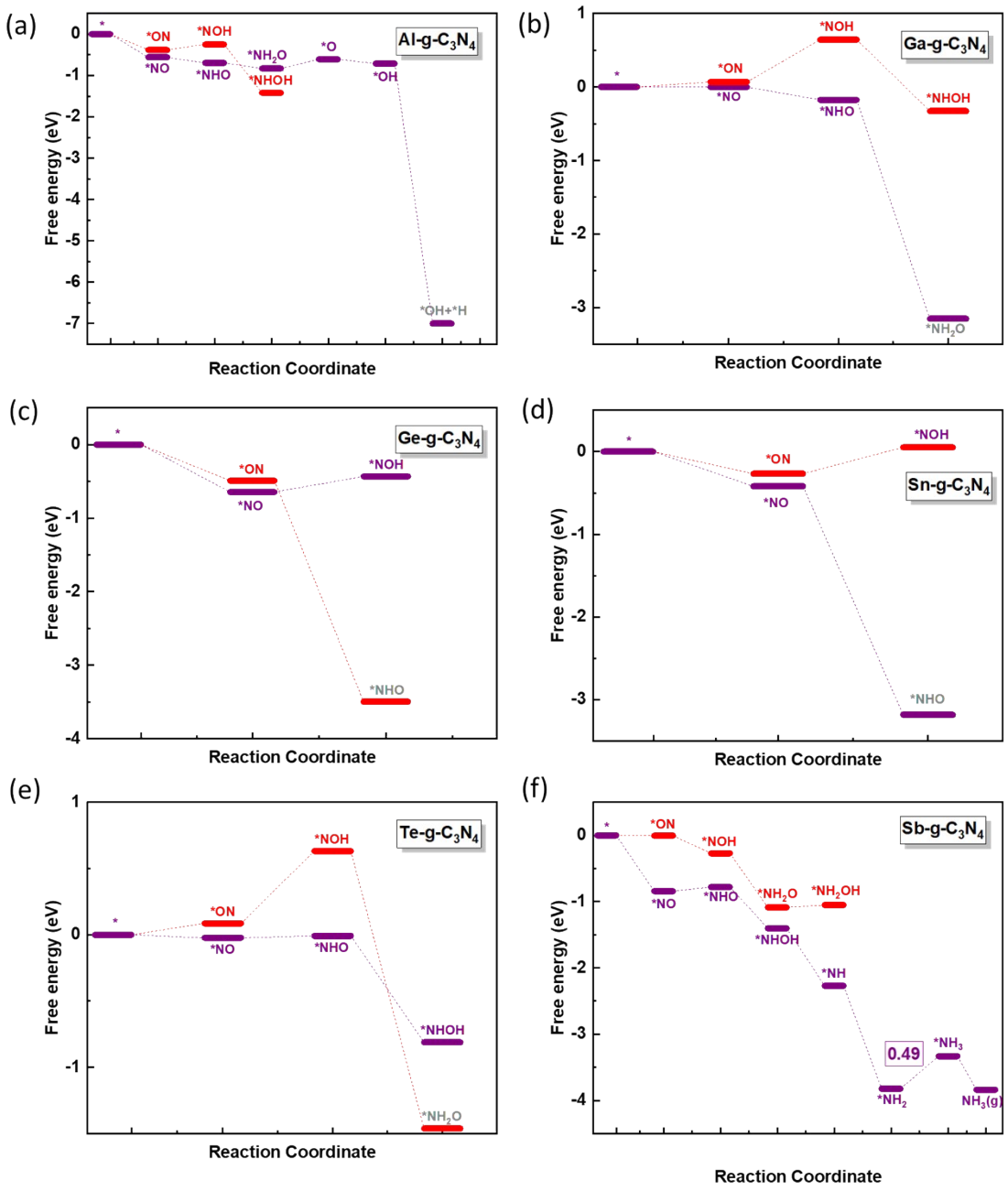

Fig S3. The Gibbs free energy changes of NORR on SAC@g-C_3N_4, including low activity or unfavourable bifurcations, all of which are excluded.

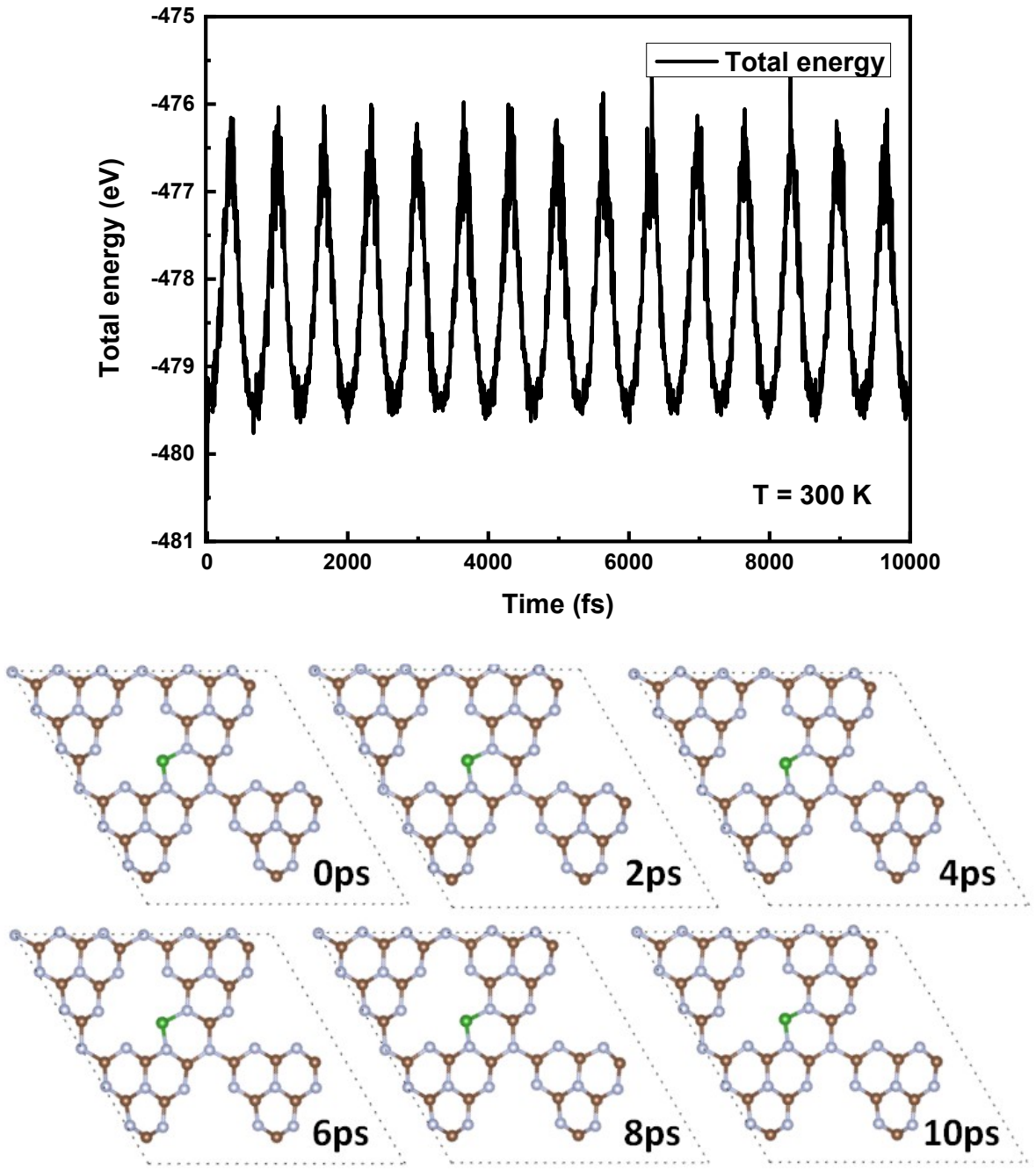

Fig S4. top: total energy evolution of B@g-C_3N_4 during AIMD simulation at 300 K; bottom: geometrical structure evolution of B@g-C_3N_4 during AIMD simulation at 300 K. Colour map: silver—N; brown—C; green—B.

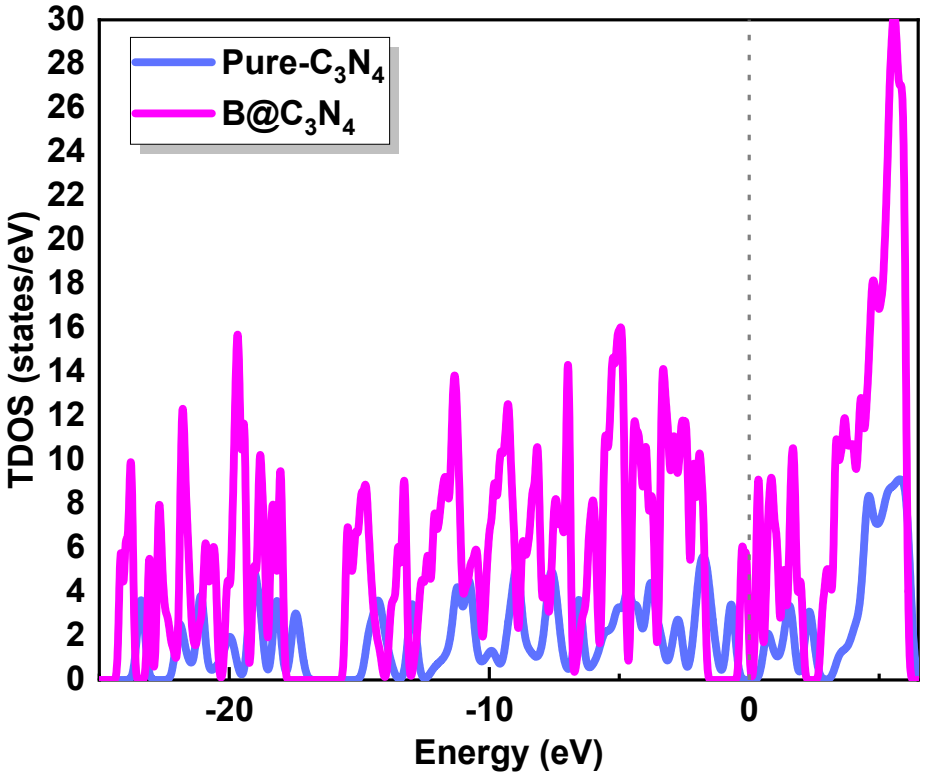

Fig S5. The TDOS comparison before and after the incorporation of B into g-C_3N_4 slab.

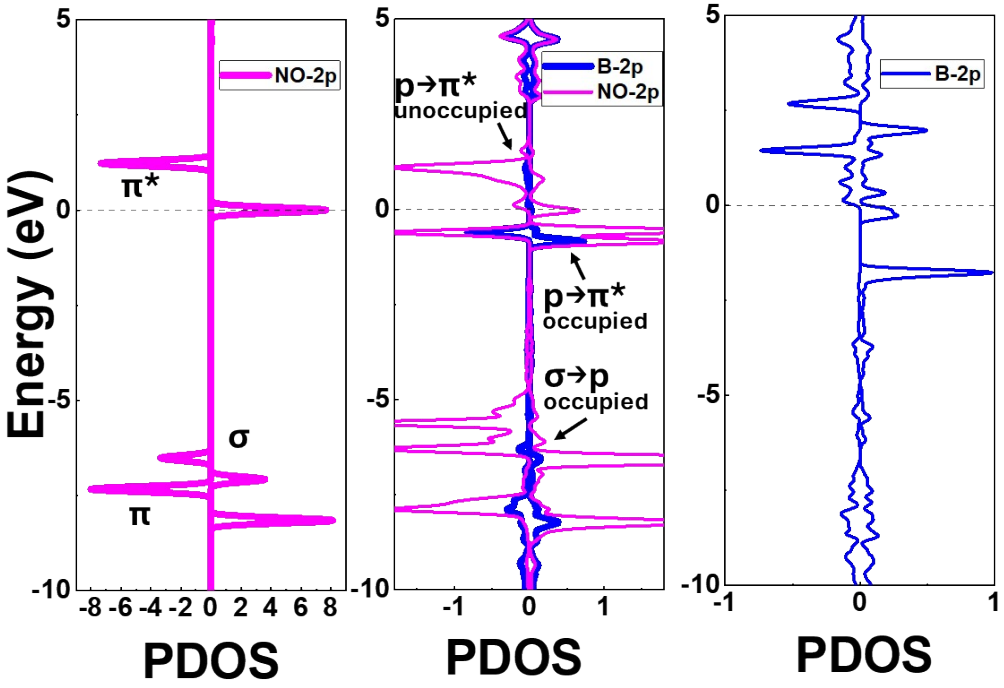

Figure S6. PDOS of p orbitals from NO, NO adsorbed on the B@g-C_3N_4 and B@g-C_3N_4.

The Fermi level is set to 0 eV.

Table S1. The comparison between gaseous NO and adsorbed NO onto the screened B@g-C_3N_4 catalyst.

Species	N-O bond length (Å)
NO(g)	1.17
B@g-C_3N_4	1.22

1. Nørskov, J. K.; Rossmeisl, J.; Logadottir, A.; Lindqvist, L.; Kitchin, J. R.; Bligaard, T.; Jonsson, H., Origin of the overpotential for oxygen reduction at a fuel-cell cathode. *The Journal of Physical Chemistry B* **2004,** *108* (46), 17886-17892.
2. Wang, V.; Xu, N.; Liu, J.-C.; Tang, G.; Geng, W.-T., VASPKIT: A user-friendly interface facilitating high-throughput computing and analysis using VASP code. *Computer Physics Communications* **2021,** *267*, 108033.